Parity-time electromagnetic diodes in a two-dimensional nonreciprocal photonic crystal

Cheng He,[1] Ming-Hui Lu,[1] Xin Heng,[2] Liang Feng,[3] and Yan-Feng Chen[1,*]

[1]*National Laboratory of Solid State Microstructures & Department of Materials Science and Engineering, Nanjing University, Nanjing 210093, People's Republic of China*

[2]*Bio-Rad Laboratories, Hercules, California 94547, USA*

[3]*Department of Electrical Engineering, California Institute of Technology, Pasadena, California 91125, USA*

(Received 1 December 2010; published 23 February 2011)

We propose a kind of electromagnetic (EM) diode based on a two-dimensional nonreciprocal gyrotropic photonic crystal. This periodic microstructure has separately broken symmetries in both parity ($\mathcal{P}$) and time-reversal ($\mathcal{T}$) but obeys parity-time ($\mathcal{PT}$) symmetry. This kind of diode could support bulk one-way propagating modes either for group velocity or phase velocity with various types of negative and positive refraction. This symmetry-broken system could be a platform to realize abnormal photoelectronic devices, and it may be analogous to an electron counterpart with one-way features.

DOI: 10.1103/PhysRevB.83.075117 PACS number(s): 42.70.Qs, 11.30.Er, 78.20.Ls

I. INTRODUCTION

The principle of symmetry is very important in the field of fundamental physical science.[1–14] For example, in optics, the one-way edge mode, as an optical counterpart to the quantum Hall effect, was reported in magneto-optical photonic crystals (MOPC's) with periodic and parity ($\mathcal{P}$) symmetries[1–3] but broken time-reversal ($\mathcal{T}$) symmetry.[4–9] In condensed-matter physics, a single surface Dirac cone, due to spin-orbit coupling, results in a topological insulator with certain topological symmetry and unbroken $\mathcal{T}$ symmetry.[10,11] Recently, a new class of optical models constructed by gain and loss materials, which have non-Hermitian Hamiltonians with both broken $\mathcal{P}$ and $\mathcal{T}$ symmetries but which obey $\mathcal{PT}$ symmetry, was demonstrated with some intriguing light-propagation properties.[12–14] In all of these cases, the existence of off-diagonal components in the Hamiltonian matrix is an essential and common mathematic structure in determining the unpaired eigenvalues. In the context of the MOPC, it has imaginary off-diagonal elements in its permeability matrix, thus it could be considered to be an excellent candidate to explore the anomalous behaviors stemming from broken symmetries in optics.

In this work, we propose a two-dimensional (2D) MOPC whose bulk modes support one-way propagation for either group velocity (V_g) or phase velocity (V_p) due to asymmetry of its photonic band structure. Contrary to the well-discussed $\mathcal{PT}$ symmetric models constructed by a periodic gain-loss medium,[12–14] this 2D MOPC separately breaks both $\mathcal{P}$ and $\mathcal{T}$ symmetries but obeys $\mathcal{PT}$ symmetry, which comes from the imaginary off-diagonal elements in its permeability matrix. We call this periodic microstructure a $\mathcal{PT}$ EM diode, which means that the transmission is unidirectional. We also show that besides the traditional one-way propagation, all four types of refraction,[15–19] that is, right-handed positive, left-handed negative, right-handed negative, and left-handed positive refraction, could be realized in a one-way feature in one MOPC for either V_g or V_p.

II. MODELS AND METHODS

The MOPC's[20,21] have demonstrated some remarkable optical performance, such as enhancement of the Faraday effect,[22,23] nonreciprocal superprisms,[24] ultracompact isolators and circulators,[25,26] and one-way chiral edge modes.[4–9] All of these effects have made use of the broken $\mathcal{T}$ symmetry. Here, we focus on a unique photonic crystal (PC) structure, namely a nonreciprocal photonic crystal (NRPC), in which both $\mathcal{P}$ and $\mathcal{T}$ symmetries are broken.[27,28] The 2D NRPC of interest is composed of a square lattice of yttrium-iron-garnet (YIG) cylinders (permittivity $\varepsilon = 15\varepsilon_0$, permeability $\mu = \mu_0$, and radius $r = 0.3a$, where a is the lattice constant) embedded in an air medium.

The one-way properties of NRPC's occur when both $\mathcal{P}$ and $\mathcal{T}$ symmetries are broken with

$$\omega(k) \neq \omega(-k), \tag{1}$$

where k and $-k$ represent a pair of counterpropagating wave vectors. To break $\mathcal{T}$ symmetry, we apply an external dc magnetic field (out of the plane along the $+z$ direction) of 1600 G to the 2D NRPC, which induces the permeability matrix to become a gyromagnetic form,

$$\overleftrightarrow{\mu} = \begin{pmatrix} \mu & i\kappa & 0 \\ -i\kappa & \mu & 0 \\ 0 & 0 & \mu_0 \end{pmatrix} = \overleftrightarrow{\mu}_d - i\kappa\, z \times \overleftrightarrow{I}, \tag{2}$$

where $\mu = 14\mu_0$ and $\kappa = 12.4\mu_0$ at 4.28 GHz.[29] $\overleftrightarrow{\mu}_d$ is the diagonal part. By reversing the external magnetic field, the off-diagonal part would flip its signs too. The gyromagnetic permeability tensor in the xy plane shows broken $\mathcal{T}$ symmetry,

$$\pi^{-1}\, \overleftrightarrow{\mu}\, \pi = \overleftrightarrow{\mu}_d + i\kappa\, z \times \overleftrightarrow{I} \neq \overleftrightarrow{\mu}, \tag{3}$$

where π is the mirror reflection transform operator. On the other hand, $\overleftrightarrow{\mu}$ has $\mathcal{P}$ symmetry, that is,

$$\sigma^{-1}\, \overleftrightarrow{\mu}\, \sigma = \overleftrightarrow{\mu}, \tag{4}$$

where σ is the spatial inversion operator. However, the $\mathcal{P}$ symmetry can be broken by using semicylinders along the y axis in each prime cell [Fig. 1(a)]. Then, the real space symmetry is broken relative to the y axis but remains intact relative to the x axis. As a result, both $\mathcal{P}$ and $\mathcal{T}$ symmetries are broken, which would result in the one-way characteristics.

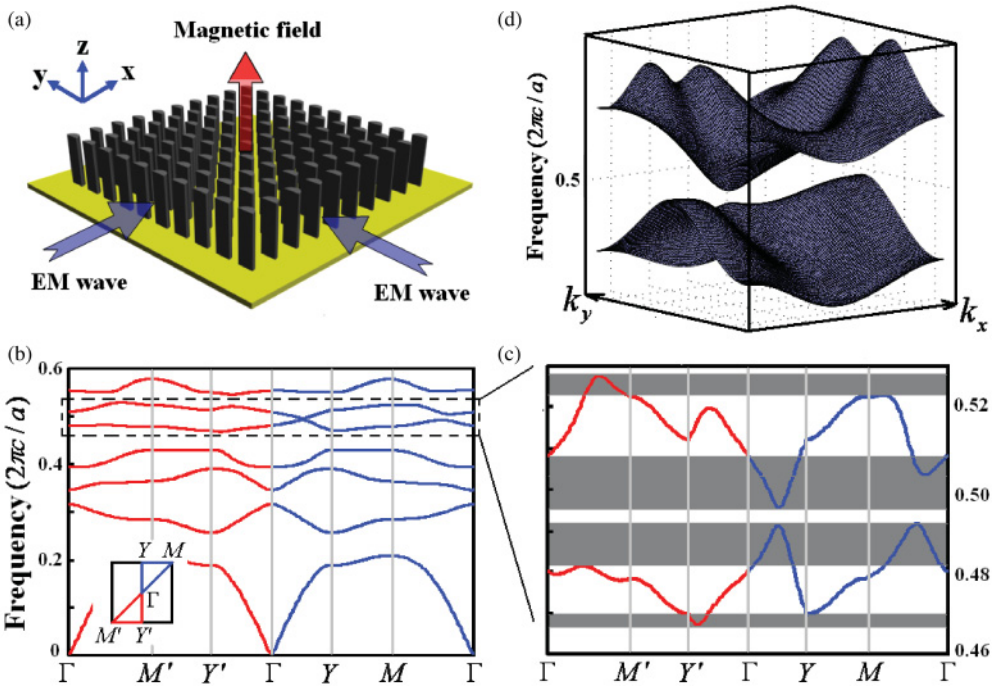

FIG. 1. (Color online) (a) Schematic of the square lattice of YIG semicylinders (black) on a copper plate (yellow) in air. (b) Band structure of YIG PC, where $\varepsilon = 15\varepsilon_0$ and $r = 0.3a$ with 1600 G + z dc external applied magnetic field ($\mu = 14\mu_0$,$\kappa = 12.4\mu_0$). The inset indicates two typical opposite high-symmetry directions in reciprocal space. (c) Zoom-in band structure of the fifth and sixth bands. The shadow regions indicate the typical one-way frequency region. The red and blue lines represent the opposite high-symmetry directions, respectively, as shown in (c). (d) Whole band structure of the fifth and sixth bands reduced in the first BZ.

For transverse magnetic (TM) modes (electric field out of plane), Maxwell's equation can be written as

$$(\Theta_0 + V)|\vec{E}\rangle = \omega^2|\vec{E}\rangle, \tag{5}$$

where $\Theta_0 = \varepsilon^{-1}(\vec{r})\nabla \times \mu^{-1}(\vec{r})\nabla\times$ is the nonmagneto part of the Hamiltonian while $V = \varepsilon^{-1}(\vec{r})\nabla \times [\overleftrightarrow{\mu}^{-1}(\vec{r}) - I\mu^{-1}(\vec{r})]\nabla\times$ represents the gyrotropic perturbation. The imaginary off-diagonal part is entirely described by V. Both Θ_0 and V are the functions of position. Under the $\hat{P}$ operation, $\hat{k} \to -\hat{k}, \hat{r} \to -\hat{r}$($\hat{r}$ and $\hat{k}$ are the position and momentum operators, respectively), the right semicylinders change to the left semicylinders, which means the incident direction of the wave is transformed to the opposite side (σ operation). Under the $\hat{T}$ operation, $\hat{k} \to -\hat{k}, \hat{r} \to \hat{r}, i \to -i$, the imaginary off-diagonal part changes sign while the position of $\hat{r}$ is kept unchanged, which is equivalent to reversing the external applied magnetic field or transforming by a mirror reflection relative to the x axis (π_x operation). Analogous to the well-discussed $\mathcal{PT}$ symmetric systems, which require the real part of the potential to be an even function of position and the imaginary part to be odd,[12,13] in this case the real part of perturbation V with a pair of counterpropagating EM waves satisfies the even function, while the imaginary part with opposite magnetic fields or with a pair of mirror-symmetric (π_x operation) incident EM waves is an odd function.[12–14]

In other words, in this NRPC there are two cases for $\mathcal{PT}$ symmetry: (i) a pair of counterincident EM waves with opposite external magnetic fields; (ii) a pair of symmetric incident EM waves relative to the y axis ($\sigma + \pi_x = \pi_y$) operation, which satisfies the even function real part of the potential and the odd imaginary part. Under this condition, the transmissions would not be one-way because the eigenvalues of Eq. (5) would come out in pairs. Furthermore, there are two cases for separately broken $\mathcal{P}$ and $\mathcal{T}$ symmetries: (i) a pair of counterincident EM waves with the same external magnetic fields; (ii) a pair of symmetric incident EM waves relative to the x axis with the same external magnetic fields. Due to this symmetry-broken system, the eigenvalues of Eq. (5) would not be in pairs anymore. By fixing a frequency ω, if the Bloch vectors k [satisfying $e^{ika}\vec{E}(r) = \vec{E}(r + a)$ for the Bloch-Floquet theorem], which indicate the direction of the incident wave, have unpaired eigenvalues, the one-way group velocity would be realized from some incident directions. Otherwise, if the Bloch vectors k have the same sign (only positive or minus), the one-way phase velocity would be realized.

The following numerical results are calculated with the finite-element method (FEM) by the COMSOL MULTIPHYSICS 3.3 program. We used its radiofrequency (rf) module in the 2D TM mode with periodic boundary conditions, and we thoroughly reduced the adverse influence from meshing errors and outer boundaries.

III. RESULTS AND DISCUSSION

A. Asymmetric band structure

When both $\mathcal{P}$ and $\mathcal{T}$ symmetries are simultaneously broken, the asymmetric band structure can be derived, as shown in

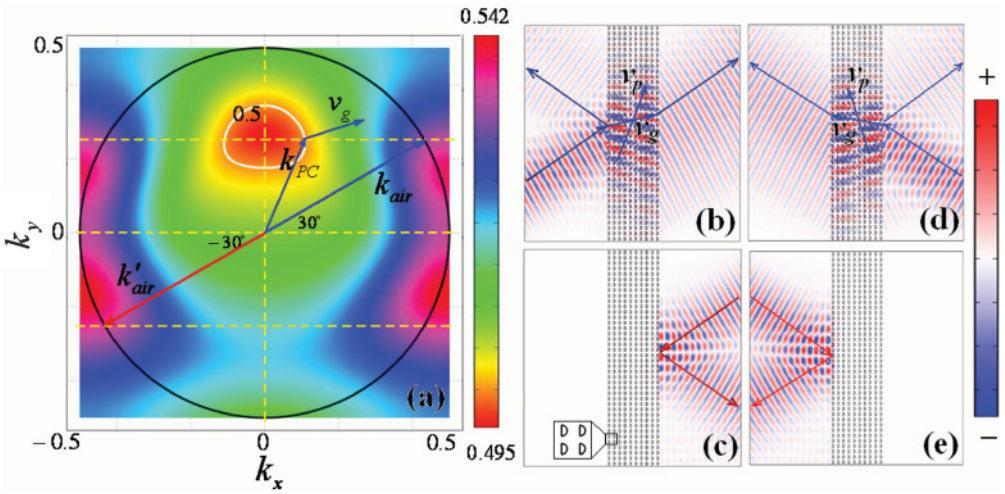

FIG. 2. (Color online) One-way propagation for group velocity with the y-cut NRPC. (a) Contour plot for the sixth band, where the white and black circles are the EFS at a frequency of $0.5(2\pi c/a)$ in the NRPC and in air, respectively. V_g and V_p with a pair of counterincident waves along the x direction are indicated by blue ($+30^\circ$) and red (-30°) arrows, respectively. The corresponding electric-field distribution is shown with (b) $+30^\circ$ from the lower left and (c) -30° from the upper right. Parts (d) and (e) are the $\mathcal{PT}$ symmetric cases corresponding to (b) and (c), respectively.

Fig. 1(b). Due to the asymmetric structure, we should choose two opposite high-symmetry directions to show the one-way characters [the inset in Fig. 1(b) indicates two typical opposite high-symmetry directions in reciprocal space]. Three things should be noticed in this dispersion relation: (i) the two sides of the Brillouin zone (BZ) center in the first four bands are almost the same; (ii) the band structures remain symmetric in YM and $Y'M'$ but are asymmetric in other directions corresponding to the center of the BZ, which stems from the fact that the k space remains symmetric relative to the k_y direction; and (iii) a pair of high-symmetry points are still equivalent points, which must have the same eigenfrequencies according to the Bloch-Floquet theorem. An enlarged picture of the fifth and sixth bands is shown in Fig. 1(c). The strongly bended dispersion curves are due to the broken symmetries, which then result in the band structures upshifting. By comparing the two sides of the center of the BZ, we identify some bump-shape and pit-shape areas in either side, which indicate the different one-way characters as shown in the shadow regions of Fig. 1(c). The whole band structure of the fifth and sixth bands in the reduced BZ is shown in Fig. 1(d). In bump-shape and pit-shape areas, the Bloch vectors are totally shifted to one side with the same sign, which means that the frequency in these regions would be one-way frequency. For example, the incident wave with some angles from the left would transmit but be completely reflected from the right independent of the angles. Large regions of the incident angle and frequency would be realized in one direction. Therefore, this 2D NRPC can provide much flexibility for the device design in terms of operating frequencies and incident directions.

Near the frequency $0.495(2\pi c/a)$ in the ΓY direction [Fig. 1(c)], the maximum and minimum values in the fifth and sixth bands, respectively, are very close. This suggests that some Dirac points may not necessarily be at the high-symmetry points.[30] Generally, in a symmetric system, the Dirac point is always located at the high-symmetry point, which indicates the linear degeneracy of two bands originating from the symmetry of the eigenfunction, that is, the symmetry of the component and lattice. In the NRPC, due to the broken symmetry of the component medium YIG, some occasional linear degeneracy might occur, causing a shift in the position away from the high-symmetry point. Actually, the one-way character with the Dirac point may make it useful and convenient to study some pseudospin and spin characters in the PC for photons and graphene for electrons, respectively.[31–33]

B. One-way group velocity

To realize the one-way group velocity, we choose the incident direction along the x direction in the y-cut NRPC. We study the one-way bulk modes of V_g in the sixth band. The equifrequency surface (EFS) is used to analyze the one-way propagation of the EM waves. As shown in Fig. 2(a), the EFS is asymmetric, in which a pit frequency ranging from about $0.495(2\pi c/a)$ to $0.505(2\pi c/a)$is enclosed with a white solid line corresponding to $k_x \in 2\pi/a \cdot [-0.15, 0.15]$ and $k_y \in 2\pi/a \cdot [0.1, 0.38]$, respectively. As an example, we choose a pair of counterpropagating incident waves with $\omega = 0.5(2\pi c/a)$ at an incident angle of $+/-30^\circ$ from the lower left and upper right, respectively, shown as blue (denoted as k) and red (k') arrows in Fig. 2(a). The white and black circles represent the EFS at a frequency of $0.5(2\pi c/a)$ in NRPC and in air, respectively. Only then can the k wave vector of the incident EM waves from $+30^\circ$ intersect the EFS of the NRPC. The k' (-30° incident) wave vector is not able to intersect the EFS, which means that due to the mismatch of the phase condition, the incident wave with -30° incident angle is totally reflected, as shown in Figs. 2(b) and 2(c).

Moreover, a pair of incident EM waves that are symmetric relative to the x axis is also nonreciprocal, while a pair of incident EM waves that are symmetric relative to the y axis can be treated as a $\mathcal{PT}$ symmetric case. Figures 2(d) and 2(e) are the $\mathcal{PT}$ symmetric cases corresponding to Figs. 2(b) and 2(c), respectively, and vice versa. In other words, the NRPC can

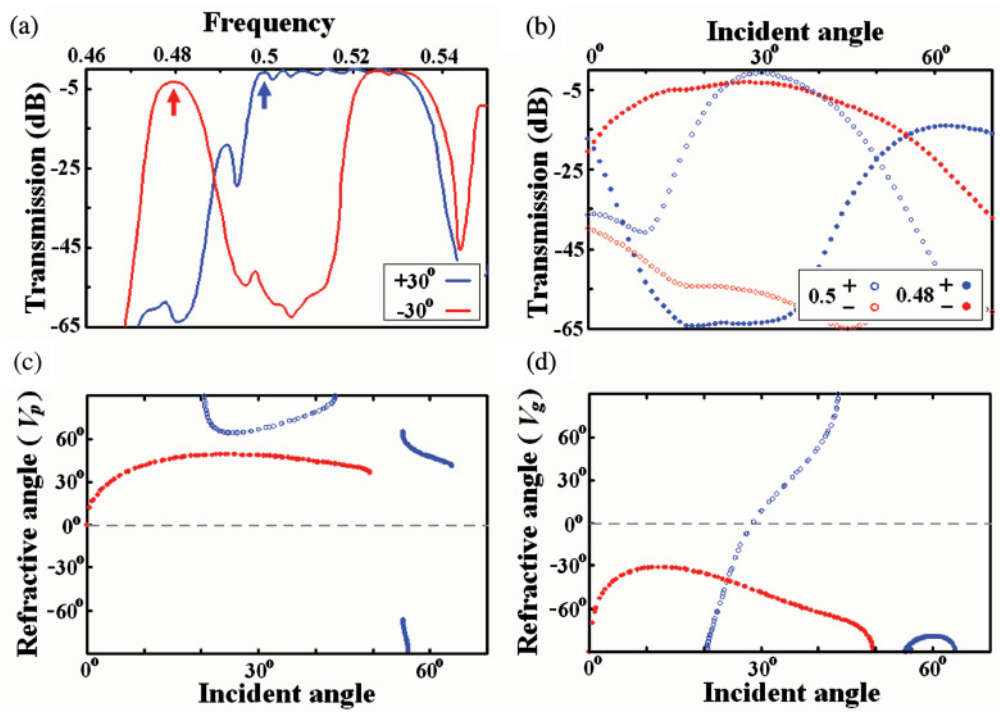

FIG. 3. (Color online) Transmission vs refraction angles with the y-cut NRPC. Blue and red indicate incident waves from the lower left (+) and the upper right (−), respectively. (a) Transmission spectra (10 layers) of $+/-30^\circ$ incident. (b) Transmission at a frequency of $0.5(2\pi c/a)$ (open circles) and 0.48 (solid dots) with various incident angles. Refractive angles of (c) V_p and (d) V_g at a frequency of $0.5(2\pi c/a)$ (open circles) and $0.48(2\pi c/a)$ (solid dots) with various incident angles.

be a lens for the upper part of the xy plane since it allows the incident waves from the lower part to transmit, while it turns out to be a mirror for the lower part, which can only get the waves to reflect from the same side of the upper incident waves. Furthermore, if the frequency is chosen in the bump frequency range of the fifth band, for example, $0.48(2\pi c/a)$, the opposite one-way direction can be realized.

We plot the angle-dependent transmission and refractive spectrum with the two opposite incident waves along the x direction in the y-cut NRPC in Fig. 3. Figure 3(a) clearly shows that $0.5(2\pi c/a)$ and $0.48(2\pi c/a)$ ($+/-30^\circ$ incident) are two prominent frequencies having different one-way features. Within a relatively broad bandwidth of $\Delta\omega/\omega \approx 5\%$, our NRPC structure shows an excellent transmission-reflection ratio, greater than 40 dB. In addition, large incident angles are allowed for one-way refraction in this case: about 20°–40° at a frequency of $0.5(2\pi c/a)$, and about 10°–50° at a frequency of $0.48(2\pi c/a)$ [Fig. 3(b)]. Figures 3(c) and 3(d) show the angles of refraction of V_g and V_p, respectively, with various incident angles, where negative V_g represents negative refraction and negative V_p indicates backward phase propagation. Due to the asymmetric EFS, various refraction types could occur in a one-way feature in this model. For instance, at a frequency of $0.48(2\pi c/a)$ with $\theta_{\text{in}} = -30^\circ$, the $V_g < 0$ means that it is the right-handed negative refraction [red solid dots in Fig. 3(d)]. More interestingly, "birefraction" would occur, that is, the coexistence of negative and positive V_p with $\theta_{\text{in}} = 53^\circ$ [blue solid dots in Fig. 3(c)].

We also calculate three typical propagating cases, as shown in Mov. S1.[34] At a frequency of $0.50(2\pi c/a)$ with incident angle $\theta_{\text{in}} = +/-23^\circ$, the propagation is the one-way right-handed negative refraction. At a frequency of $0.48(2\pi c/a)$ with incident angle $\theta_{\text{in}} = +/-30^\circ$, the propagation is also right-handed negative refraction, but with different one-way characters.

In other words, the case in Fig. 2 is the one-way right-handed positive refraction. On the other hand, the one-way right-handed negative refraction can be achieved at the same frequency with a smaller incident angle, that is, $\theta_{\text{in}} < 28^\circ$ [blue open circles in Figs. 3(c) and 3(d)]. If we choose the operating frequency region in the fifth band, a bump-shaped region would allow us to construct one-way left-handed positive and one-way left-handed negative refraction, respectively.

C. Refractive types

In general, there are two key factors to determine the optical refraction: one is the conservation of the wave vector, $k_{||}^{\text{PC}} = k_{||}^{\text{incident}}$, the other is the causality of the wave propagation, $V_{g\perp}^{\text{PC}} \cdot V_{g\perp}^{\text{incident}} > 0$, where $\perp$ and $||$ represent the directions perpendicular to and parallel to the boundary of the NRPC, respectively. For these reasons, only the right intersecting point in Fig. 2(a) could be considered as a physical reality. It should be noticed that the directions of $k_{\perp}^{\text{PC}}$(indicating the forward or backward phase propagation) and $V_{g||}^{\text{PC}}$(indicating the positive or negative refraction) could not be restricted. Therefore, there are a total of four types of refraction in this system. Here, a general table was used to categorize these four types of refraction, as shown in Fig. 4. In addition to the well-known right-handed positive (upper left part of Fig. 4) and

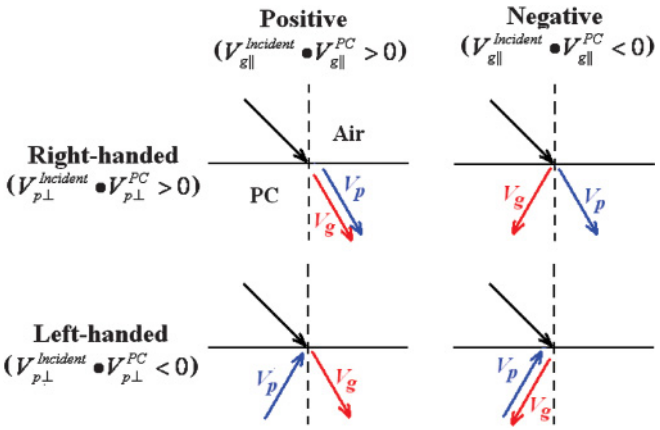

FIG. 4. (Color online) Category of four types of refraction. $\perp$ and || represent the directions normal to and along the boundary between air and the NRPC, respectively.

left-handed negative (lower right part of Fig. 4) refractions, in the symmetry-broken system the group velocity and phase velocity were often separated into different directions to form the left-handed positive (lower left part of Fig. 4) and right-handed negative (upper right part of Fig. 4) refractions. The advantage of this category is that we can clearly distinguish that the negative refraction is decided by the sign of $V_{g||}^{\text{incident}} V_{g||}^{\text{PC}}$ while the backward phase propagation is decided by the sign of $V_{p\perp}^{\text{incident}} V_{p\perp}^{\text{PC}}$. This category can help us to understand that positive refraction can also amplify the evanescent wave, while the forward phase propagation can also realize the negative refraction.[18]

By using these criteria, the refractive waves in Fig. 2(b) are cataloged as the right-handed and positive refraction. All four types of refraction can be achieved with the one-way character for V_g in this model too. Due to the strong bending of EFS, the refractive angle would vary rapidly when sweeping the incident angle. Moreover, flipping the external applied magnetic field could reverse the direction of one-way propagation. This property would have great potential in preparing some new optoelectronic devices, such as superprisms and optical switches.

D. One-way phase velocity

To discuss the one-way phase propagation, we change the incident direction along the y direction in the x-cut NRPC. The waves operating in the same pit frequency domain as in the previous discussion would propagate with the one-way features not for V_g but for V_p. As shown in Fig. 5(a), we choose a pair of counterincident waves with angle $+/-10^\circ$ along the y direction at a frequency of $0.5(2\pi c/a)$. The blue and red arrows correspond to $+10^\circ$ incident and -10° incident waves from the lower left and upper right, respectively. Each of the counterincident waves would have the same two intersecting points. Due to the causality, these counterincident waves would choose different intersecting points to propagate. The EM waves show right-handed refraction for a $+10^\circ$ incident wave and left-handed refraction for a -10° incident wave, as shown in Figs. 5(b) and 5(c), respectively. When $\theta_{\text{in}} < 12^\circ$, V_p stays positive along the $+y$ axis. To realize the one-way phase velocity in the NRPC, two conditions should be satisfied: (i) both $\mathcal{P}$ and $\mathcal{T}$ symmetries must be broken to cause the unpaired Bloch vectors; (ii) these unpaired Bloch vectors should have the same sign (i.e., the EFS should be totally shifted to one side), which means that the symmetry breaking should be large enough.

For the one-way property of V_p, we plot the angles of refraction of V_g and V_p, respectively, versus various incident angles along the y axis in the x-cut NRPC in Fig. 6. The different signs of V_p represent different handedness (left-handed or right-handed), while the different signs of V_g

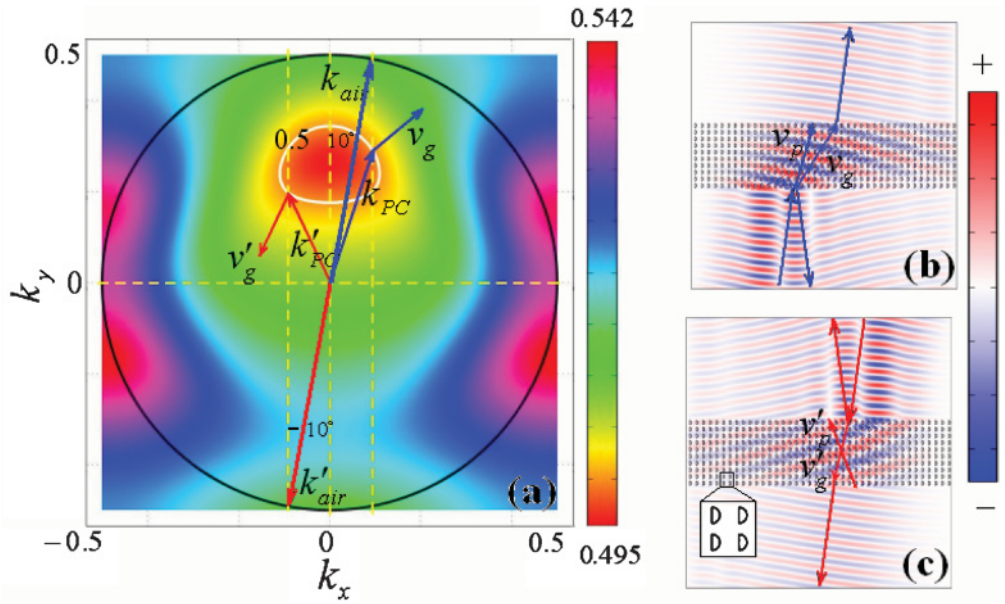

FIG. 5. (Color online) One-way propagation for phase velocity with the x-cut NRPC. (a) Contour plot for the sixth bands with $+/-10^\circ$ incident angle along the y direction at a frequency of $0.5(2\pi c/a)$. The corresponding electric-field distribution is shown with (b) $+10^\circ$ from the lower left and (c) -10° from the upper right.

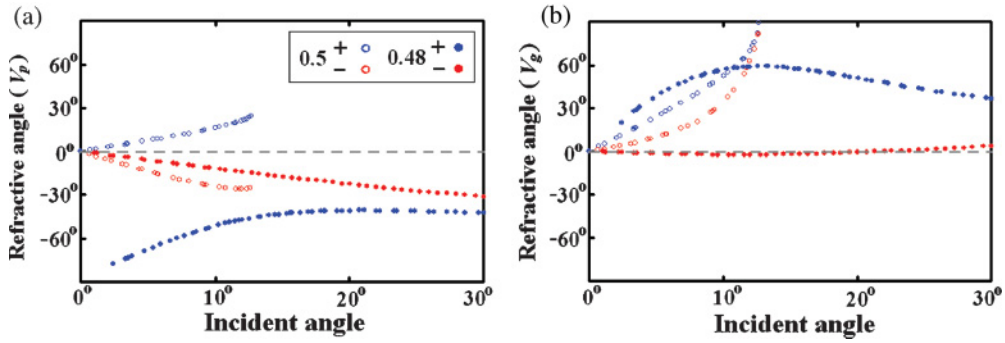

FIG. 6. (Color online) Refractive angles with the x-cut NRPC. Blue and red indicate incident waves from the lower left (+) and upper right (−), respectively. Refractive angles of (a) V_p and (b) V_g at a frequency $0.5(2\pi c/a)$ (open circles) and $0.48(2\pi c/a)$ (solid dots) with various incident angles.

indicate refraction types (negative or positive). Frequency $0.5(2\pi c/a)$ with less than 12° incident angle is the typical one-way range for V_p. At a frequency of $0.48(2\pi c/a)$ with $\theta_{\text{in}} < 20°$, a pair of counterincident EM waves would both propagate left-handed but with different refractive types [solid line in Figs. 6(a) and 6(b)]: positive refraction for the incident wave from the lower left, negative refraction for the incident wave from the upper right. Moreover, all four types of refraction could be realized with one-way character for V_p. By reversing the external magnetic field, the one-way V_p would be reversed, which also obeys $\mathcal{PT}$ symmetry. These properties could be applied in some photoelectronic devices such as a phase filter and a one-way phase compensator.

Similarly, we choose three typical propagating cases as shown in Mov. S2.[35] At a frequency of $0.50(2\pi c/a)$ with normal incidence, the propagations of the counterincident waves have the same direction of V_p but with opposite handedness: right-handed for the incident wave from the lower part, left-handed for the incident wave from the upper part. At a frequency $0.48(2\pi c/a)$ with incident angle $\theta_{\text{in}} = +/-30°$, the one-way direction of V_p is reversed: left-handed positive refraction for the incident wave from the lower part, right-handed positive refraction for the incident wave from the upper part.

Recently, a time-reversal method was proposed to realize a perfect lens with negative refraction by four-wave mixing.[19] The evanescent wave without carrying energy can be collected for perfect imaging due to the backward phase propagation. In the NRPC (Fig. 5), the counterincident waves would have opposite handedness, which would have a one-way phase-compensation effect in only one direction. This means that the amplification of the evanescent wave in a PC may not necessarily be associated with $\mathcal{T}$ symmetry. Therefore, the NRPC provides an alternative device model to realize the one-way perfect lens in a $\mathcal{T}$ symmetry-broken system.

E. Composite structure

As mentioned earlier, the one-way operating frequency is about $0.5(2\pi c/a)$. From an experimental point of view, the lattice constant should be chosen about 3.5 cm. The one-way frequency is near 4.28 GHz. Although the structure under consideration has one-way features in the flat fifth and sixth bands, the wavelength is about double the lattice constant, which may not be difficult to measure in experiment. On the other hand, a composite model could lower the one-way bands, as shown in Fig. 7. The band structure of a composite NRPC is shown in the inset [Fig. 7(a)], where the left semicylinder is a dielectric medium ($\varepsilon = 16\varepsilon_0$), the right semicylinder is

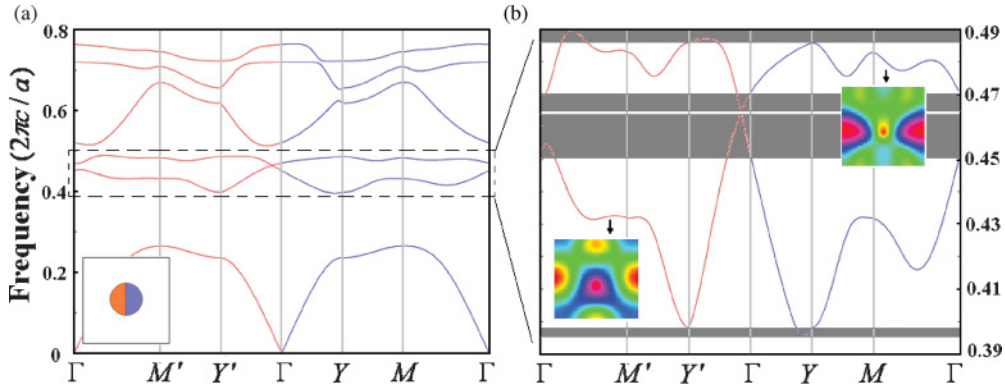

FIG. 7. (Color online) (a) Band structure of composite PC (inset), where the left semicylinder is the dielectric medium ($\varepsilon = 16\ \varepsilon_0$), the right semicylinder is YIG ($\varepsilon = 15\ \varepsilon_0$, $\mu = 14\ \mu_0$, $\kappa = 12.4\ \mu_0$), and $r = 0.3a$. (b) Zoom-in band structure of the second and third bands. The shadow regions indicate the typical one-way frequency region. The red and blue lines represent the opposite high-symmetry directions. Insets are the EFS of the second and third bands.

YIG ($\varepsilon = 15\varepsilon_0$, $\mu = 14\mu_0$,$\kappa = 12.4\mu_0$), and $r = 0.3a$. The one-way features occur in the second and third bands. The enlarged band structure is shown in Fig. 7(b). The shadow regions indicate the typical one-way frequency region. The red and blue lines represent the opposite high-symmetry directions. Insets are the EFS of the second and third bands. By enlarging the condition of the asymmetry, the region of one-way frequency would be enlarged correspondingly. With regard to the measurement of one-way V_p, the changes of phase can be determined by increasing or decreasing the number of periods of NRPC's. The one-way phase propagation may be achieved by comparing the different phase changes of two counterincident waves.

IV. CONCLUSIONS

These effects can be attributed to the non-Hermitian eigenequation. With broken $\mathcal{P}$ and $\mathcal{T}$ symmetries, the Bloch vectors could have unpaired real values for the same frequency. Compared to the one-way edge mode with $\mathcal{P}$ symmetry,[4–9] the eigenequation is Hermitian, and the real parts of the Bloch vectors are always equal with opposite signs.[9] This means that they cannot support the one-way bulk mode. On the other hand, due to the periodicity of the NRPC, where the eigenvalues of high-symmetry points remain the same, the intersections of the normal incident wave vector would result in a pair corresponding to forward and backward energy flow, respectively. Therefore, one-way propagation of V_g would never happen for normal incident waves in periodic cases. However, the V_p can be one-way for normal incidence, which can be treated as another novel phenomenon (phase diode) stemming from the broken $\mathcal{P}$ and $\mathcal{T}$ symmetries.

In summary, we proposed a 2D NRPC with broken $\mathcal{P}$ and $\mathcal{T}$ symmetries simultaneously. The asymmetry of $\mathcal{P}$ and $\mathcal{T}$ would bring more parameters in the band engineering to control and realize the $\mathcal{PT}$ EM diodes, which could show one-way features either for V_g or V_p due to the NRPC's asymmetric band structure. Four types of refraction cases could be realized in one NRPC, depending on the operating frequency and incident angle. These properties may have great potential applications in optoelectronic phase-control devices, such as optical isolators, optical switches, and phase compensators. Using such a macrosystem of NRPC's with $\mathcal{PT}$ symmetry, we have the potential to realize some exotic quantum phenomena that can mimic electronic quantum effects, such as the optical counterpart of quantum spin Hall effects or the optical counterpart of topological insulators.

ACKNOWLEDGMENTS

The work was supported jointly by the National Basic Research Program of China (Grant No. 2007CB613202) and the National Nature Science Foundation of China (Grant No. 50632030). We also acknowledge the support from the Nature Science Foundation of China (Grant No. 10874080) and the Nature Science Foundation of Jiangsu Province (Grant No. BK2009007).

*yfchen@nju.edu.cn

[1] S. John, Phys. Rev. Lett. **58**, 2486 (1987).
[2] E. Yablonovitch, Phys. Rev. Lett. **58**, 2059 (1987).
[3] J. D. Joannopoulos, R. D. Meade, and J. N. Winn, *Photonic Crystals: Modeling the Flow of Light* (Princeton University Press, Princeton, NJ, 1995).
[4] F. D. M. Haldane and S. Raghu, Phys. Rev. Lett. **100**, 013904 (2008).
[5] Z. Wang, Y. D. Chong, J. D. Joannopoulos, and M. Soljačić, Phys. Rev. Lett. **100**, 013905 (2008).
[6] Z. Wang, Y. D. Chong, J. D. Joannopoulos, and M. Soljačić, Nature (London) **461**, 772 (2009).
[7] X. Ao, Z. Lin, and C. T. Chan, Phys. Rev. B **80**, 033105 (2009).
[8] C. He, X. L. Chen, M. H. Lu, X. F. Li, W. W. Wan, X. S. Qian, R. C. Yin, and Y. F. Chen, Appl. Phys. Lett. **96**, 111111 (2010).
[9] C. He, X. L. Chen, M. H. Lu, X. F. Li, W. W. Wan, X. S. Qian, R. C. Yin, and Y. F. Chen, J. Appl. Phys. **107**, 123117 (2010).
[10] H. Zhang, C. X. Liu, X. L. Qi, X. Dai, Z. Fang, and S. C. Zhang, Nature Phys. **5**, 438 (2009).
[11] Y. Xia, D. Qian, D. Hsieh, L. Wray, A. Apl, H. Lin, A. Bansil, D. Grauer, Y. S. Hor, R. J. Cava, and M. Z. Hasan, Nature Phys. **5**, 398 (2009).
[12] K. G. Makris, R. El-Ganainy, D. N. Christodoulides, and Z. H. Musslimani, Phys. Rev. Lett. **100**, 103904 (2008).
[13] C. E. Rüter, K. G. Makris, R. El-Ganainy, D. N. Christodoulides, M. Segev, and D. Kip, Nature Phys. **6**, 192 (2010).
[14] P. M. Rinard and J. W. Calvert, Am. J. Phys. **39**, 753 (1971).
[15] V. G. Vesselago, Sov. Phys. Usp. **10**, 509 (1968).
[16] L. Feng, X. P. Liu, Y. F. Tang, Y. F. Chen, J. Zi, S. N. Zhu, and Y. Y. Zhu, Phys. Rev. B **71**, 195106 (2005).
[17] N. H. Shen, Q. Wang, J. Chen, Y. X. Fan, J. P. Ding, H. T. Wang, Y. Tian, and N. B. Ming, Phys. Rev. B **72**, 153104 (2005).
[18] L. Feng, X. P. Liu, M. H. Lu, Y. B. Chen, Y. F. Chen, Y. W. Mao, J. Zi, Y. Y. Zhu, S. N. Zhu, and N. B. Ming, Phys. Rev. Lett. **96**, 014301 (2006).
[19] J. B. Pendry, Science **322**, 71 (2008).
[20] I. L. Lyubchanskii, N. N. Dadoenkova, M. I. Lyubchanskii, E. A. Shapovalov, and Th. Rasing, J. Phys. D **36**, R277 (2003).
[21] M. Inoue, R. Fujikawa, A. Baryshev, A. Khanikaev, P. B. Lim, H. Uchida, O. Aktsipetrov, A. Fedyanin, T. Murzina, and A. Granobsky, J. Phys. D **39**, R151 (2006).
[22] R. Wolfe, R. A. Lieberman, V. J. Frantello, R. E. Scotti, and N. Kopylov, Appl. Phys. Lett. **56**, 426 (1990).
[23] M. Inoue, K. Arai, T. Fujii, and M. Abe, J. Appl. Phys. **83**, 6768 (1998).
[24] I. Bita and E. L. Thomas, J. Opt. Soc. Am. B **22**, 1199 (2005).
[25] Z. Wang and S. Fan, Opt. Lett. **30**, 1989 (2005).
[26] Z. Wang and S. Fan, Appl. Phys. B **81**, 369 (2005).

[27]Z. Yu, Z. Wang, and S. Fan, Appl. Phys. Lett. **90**, 121133 (2007).

[28]M. Vanwolleghem, X. Checoury, W. Smigaj, B. Gralak, L. Magdenko, K. Postava, B. Dagens, P. Beauvillain, and J. M. Lourtioz, Phys. Rev. B **80**, 121102(R) (2009).

[29]D. M. Pozar, *Microwave Engineering*, 2nd ed. (Wiley, New York, 1998).

[30]S. L. Yu, J. X. Li, and L. Sheng, Phys. Rev. B **80**, 193304 (2009).

[31]R. A. Sepkhanov, J. Nilsson, and C. W. J. Beenakker, Phys. Rev. B **78**, 045122 (2008).

[32]K. S. Novoselov, A. K. Geim, S. V. Morozov, D. Jiang, M. I. Katsnelson, I. V. Grigorieva, S. V. Dubonos, and A. Firsov, Nature (London) **438**, 197 (2005).

[33]Y. Zhang, Y. W. Tan, H. L. Stormer, and P. Kim, Nature (London) **438**, 201 (2005).

[34]See supplemental material at [http://link.aps.org/supplemental/10.1103/PhysRevB.83.075117] Movies of three typical onw-way V_g cases.

[35]See supplemental material at [http://link.aps.org/supplemental/10.1103/PhysRevB.83.075117] Movies of three typical onw-way V_p cases.